International Journal of Thermal Sciences 153 (2020) 106365

Contents lists available at ScienceDirect

International Journal of Thermal Sciences

journal homepage: http://www.elsevier.com/locate/ijts

Numerical study on thermal-hydraulic performance and exergy analysis of laminar oil flow in a circular tube with fluid exchanger inserts

Peng Liu, Zhimin Dong, Jinyi Lv, Feng Shan, Zhichun Liu, Wei Liu *

School of Energy and Power Engineering, Huazhong University of Science and Technology, Wuhan, 430074, China

ARTICLE INFO

Keywords:
Fluid exchanger inserts
Heat transfer enhancement (HTE)
Laminar flow
Exergy analysis

ABSTRACT

A novel tube insert, fluid exchanger inserts, is proposed and numerically investigated for enhancing convective heat transfer of laminar oil flow in a circular tube. Effects of parameters including diameter ratio and number of inserts on convective heat transfer performance are also investigated. In the present work, servotherm medium oil is selected as the working fluid. It is found that the heat transfer performance is effectively enhanced as the thermal boundary layer is completely destroyed when the fluid passes through the fluid exchanger inserts. The Nusselt number and friction factor of the tube with fluid exchanger inserts are enhanced to 1.63–2.69 and 1.72–7.01 times that of the plain tube, respectively. Thus, the performance evaluation criterion ranges from 1.24 to l.62. Moreover, exergy analysis is conducted to appraise the thermodynamic performance of the tube with fluid exchanger inserts. It is found that the exergy efficiency of the enhanced tube is improved by 0.3%–1.9% compared to the plain tube.

1. Introduction

Heat exchangers, which are the indispensable devices for heat exchanging, are widely applied in engineering areas and industrial fields. To improve the thermal transfer performance and save energy, heat transfer enhancement techniques (HTET) are necessary and widely investigated. Generally, according to whether external power input is required or not, the HTET are classified into active techniques and passive techniques [1]. The passive method is more frequently adopted in practical application because of its low cost and easy maintenance.

Heat exchange tube is the basic component in most heat exchangers. Until now, a large number of passive HTETs for heat exchange tube including extended or roughened surface and tube inserts have been proposed in literature [2], in which tube inserts are most frequently researched and used in engineering application due to its easy installation and low cost. Twisted tape inserts, which can increase the fluid velocity and generate swirling flow in tube, is the most widely studied HTET for tube flow and heat transfer. Since Manglik et al. [3,4] reported experimental researches on performance of convective heat transfer in a tube with twisted-tape inserts, twisted tape inserts has drawn extensive attention and numerous modifications of twisted tape has been proposed and investigated. Some modifications [5–8] aim to dramatically reduce the pressure drop in the tube without much reduction in heat transfer. For example, Saha et al. [5] reported that compared to full-length twisted-tape, a regularly spaced twisted-tape can substantially reduce the flow resistance. Guo et al. [6] reported a numerical study on the thermo-hydraulic performance of tube with center-cleared twisted tape. It was found that the center-cleared twisted tape avoids disturbing the high-speed fluids in the center of the tube. Thus, compared to the traditional twisted tape, the flow resistance can be apparently reduced and the thermal performance factor can be enhanced by 7–20%. Other modifications aim to further enhance the heat transfer coefficient, such as different cut twisted tape [9,10], broken twisted tape[11] and serrated twisted tape [12]. Helical screw tapes [13–15] are the other widely studied tube inserts, which generally form a single large swirling flow in tube so as to enhance heat transfer. Sivashanmugam [13] reported an experimental study on convective heat transfer performance of helical screw-tape insert with core-rod in a circular tube. While Zhang et al. [14] conducted a numerical investigation on the thermo-hydraulic performance of tube fitted with helical screw-tape insert without core-rod. The third widely investigated tube inserts, coiled wire and its modifications [16–18], which is designed to disturb and reduce the thermal boundary layer, have been reported to achieve substantial enhancement in thermo-hydraulic performance.

In recent years, a great number of new/novel inserts and vortex generators have been proposed for enhancing convective heat transfer in

* Corresponding author.
E-mail address: w_liu@hust.edu.cn (W. Liu).

https://doi.org/10.1016/j.ijthermalsci.2020.106365
Received 18 January 2019; Received in revised form 17 January 2020; Accepted 6 March 2020
Available online 12 March 2020
1290-0729/© 2020 Elsevier Masson SAS. All rights reserved.

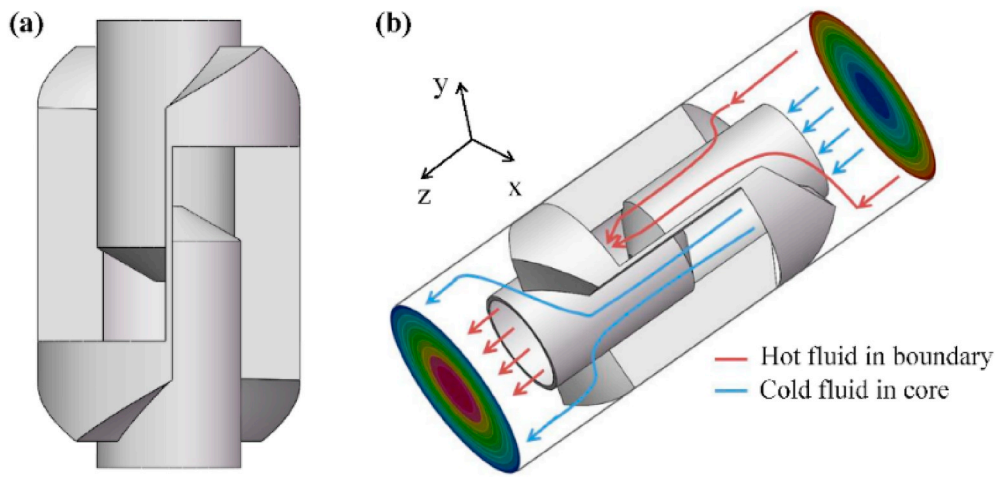

Fig. 1. (a) Schematic of the fluid exchanger insert, (b) the desired mechanism of HTE in circular tube with fluid exchanger inserts.

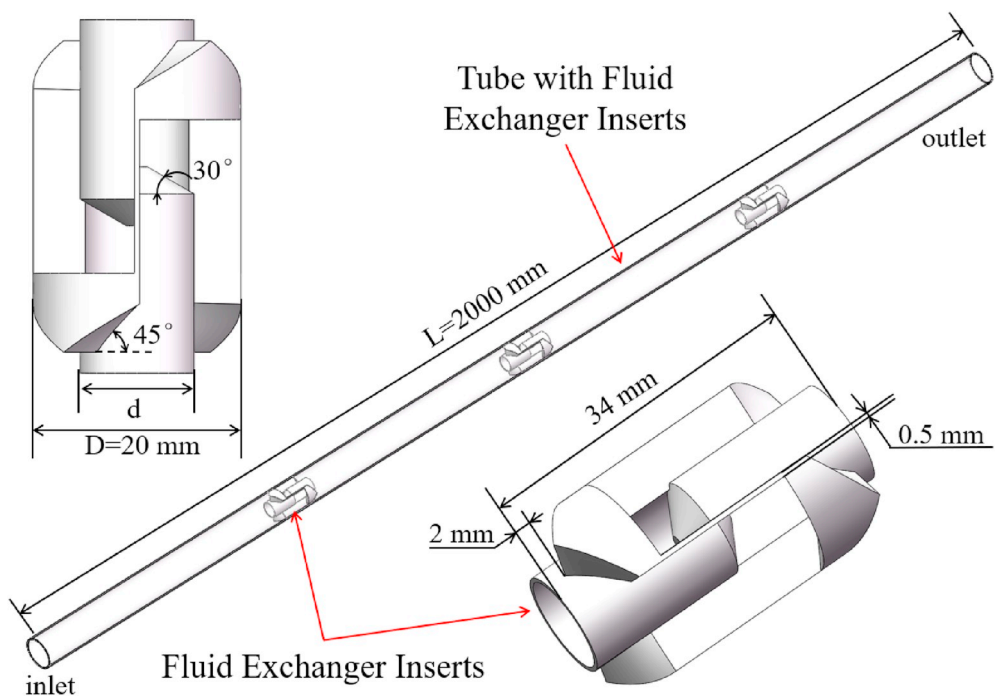

Fig. 2. Physical model and geometrical parameters of a tube fitted with fluid exchanger inserts used in the simulation.

tube flow[19]. Lei [20] and Agung [21] proposed two different delta-winglet tape inserts, respectively. This type of inserts divides the tube into two semi-circular flow channels by straight tape and generates vortexes in each semi-circular flow channel by the delta wing and thus provides improvement of convective heat transfer. Sompol et al. [22] reported a great improvement of overall heat transfer performance of tube by using curved-winglet tapes. Zhu et al. [23] conducted a numerical study on the performance of a novel wavy-tape insert. They found that vortices were formed inside the tube and overall thermo-hydraulic performance was improved up to 1.82 times of plain tube. A class of vortex generators is designed by attaching different structures such as conical strips [24,25], louvered strips [26,27], winglets [28,29], drainage structure [30] and other novel structures [31–33]. This type of vortex generators has lower flow resistance and more sufficient mixing of fluid than twisted tape. Thus, they can achieve better thermal performance than twisted tape. Cao et al. proposed a conical-mesh inserts and conducted a numerical investigation. They found that this insert can increase the fluid velocity and velocity gradient near tube wall and thus reduce thermal boundary layer. A small pipe inserts was proposed and numerically investigated for HTE in tube by Tu et al. [34]. They found that the small pipe inserts can direct the cold fluid in the center of the tube to the tube wall.

Based on survey of literature, it is found that the existing tube inserts for HTE only inhibit the thermal boundary layer by disturbing the fluid or/and increasing fluid mixing. However, what is the limit of convective heat transfer enhancement in tube flow and how to approach or reach this limit is still not clear. For non-slip walls, the underlying fluid closest to the wall is almost stationary. Therefore, the heat transfer in this fluid layer is dominated by heat conduction of the fluid. Based on Fourier's law, increasing the temperature gradient of the fluid near the wall is the key to enhancing heat transfer, since the thermal conductivity of the fluid is almost constant. Thus, the thermal boundary layer developed near the tube wall is the essential barrier to heat transfer and avoiding the formation of a thermal boundary layer completely is the limit for

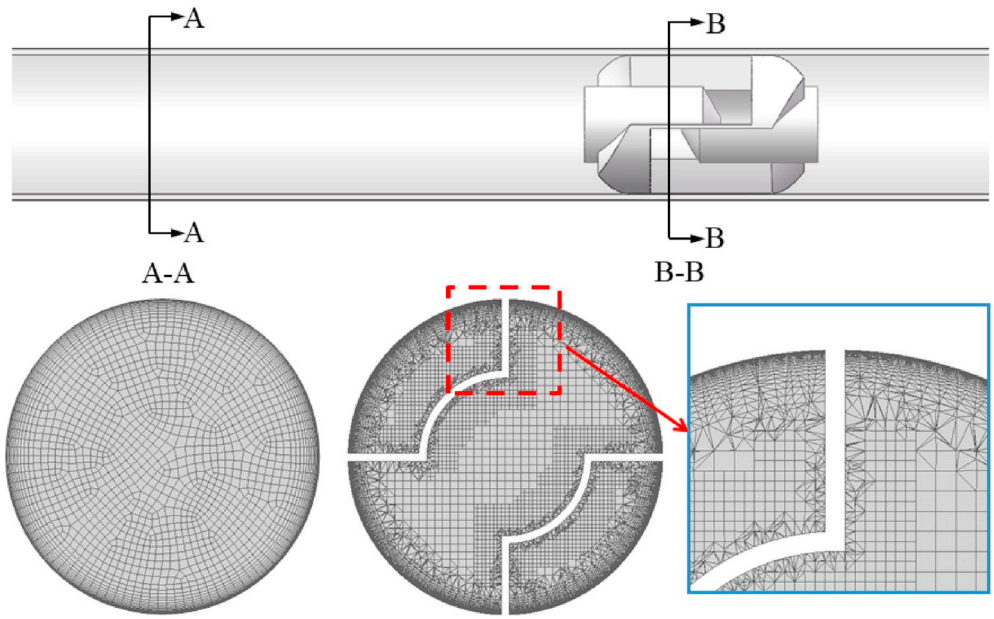

Fig. 3. Grid system.

Table 1
Grid independence test.

	Grid size	*Nu*	Error(*Nu*)	*f*	Error(*f*)
Model-I	8,035,390	31.0549	8.62%	0.6593	7.17%
Model-II	13,079,797	28.5908	1.46%	0.6152	0.85%
Model-III	18,102,149	28.1794	–	0.6101	–

Table 2
Relative errors between calculation results and values predicted by correlations for *Nu* and *f*.

Re	Calculation results		Values predicted by Eqs.		Relative errors	
	Nu	f	*Nu* (Eq. (12))	*f* (Eq. (13))	Nu	f
100	10.17	0.6574	11.84	0.6409	−14.1%	2.6%
200	12.68	0.3353	14.96	0.3205	−15.2%	4.6%
300	14.47	0.2279	17.14	0.2136	−15.6%	6.7%
400	15.92	0.1742	18.88	0.1602	−15.7%	8.7%
500	17.15	0.1412	20.35	0.1282	−15.7%	10.2%

heat transfer enhancement. Thus, if the thermal boundary layer could be completely destroyed, the convective heat transfer coefficient would be dramatically enhanced. For this purpose, a novel fluid exchanger insert, as shown in Fig. 1 (a), is proposed for HTE in tube flow. It is expected that when the fluid flow through the fluid exchanger insert, the cold fluid in the center of the tube and the hot fluid near the tube wall will be completely exchanged, as shown in Fig. 1 (b). Consequently, the thermal boundary layer is expected to be completely destroyed and the convective heat transfer coefficient is expected to be substantially enhanced. In addition, exergy analysis is also conducted to appraise the performance of the inserts.

2. Physics model description

Physical model and geometrical parameters of a tube fitted with fluid exchanger inserts investigated in this study is shown in Fig. 2. The fluid exchanger insert is a symmetrical structure, which divides the tube into an annulus channel and a central circular channel (with diameter *d*). When the fluid pass through the insert, the fluid in the annulus channel and central circular channel will exchange the location. The full length of tube in this study 2000 mm and its inner diameter(*D*) is 20 mm and some other geometrical parameters are marked in Fig. 2. Three values of the diameter ratio ($DR = d/D$ = 0.4, 0.5, 0.6) and tube with different number of inserts (N = 3, 4 and 5) were investigated to examine the influence of the geometric parameter on thermo-hydraulic performance.

3. Calculation model

3.1. Governing equations and boundary conditions

The flow in the present work is assumed to be three-dimensional, laminar and steady. In addition, to simplify the calculation, some assumptions are adopted: (1) the fluid is incompressible, continuous and isotropic; (2) the inserts is stiff and its vibration is ignored; and (3) heat conduction of the inserts is neglected. The governing equations for continuity, momentum and energy are given as Eqs. (1)–(3).

$$\frac{\partial(\rho u_i)}{\partial x_i} = 0 \quad (\mathrm{i} = 1 \sim 3) \tag{1}$$

$$\frac{\partial(\rho u_i u_j)}{\partial x_i} = -\frac{\partial P}{\partial x_i} + \frac{\partial}{\partial x_j}\left[\mu\left(\frac{\partial u_i}{\partial x_j} + \frac{\partial u_j}{\partial x_i}\right)\right] \quad (\mathrm{j} = 1 \sim 3) \tag{2}$$

$$\frac{\partial}{\partial x_i}\left(\rho u_i C_p T - \lambda \frac{\partial T}{\partial x_i}\right) = 0 \tag{3}$$

In the present work, servotherm medium oil [35] is selected as the working fluid, whose temperature-dependent properties are defined as formulas below, where T is the fluid temperature in °C. Uniform temperature and velocity are applied at the inlet. The fluid inlet temperature is set to 333.15 K (60 °C). The mean velocity of the fluid ranges from 0.076 to 0.38 m/s and the corresponding Reynolds number is located from 100 to 500. A constant temperature of 353.15 K is adopted for the tube inner wall. An outflow condition is used at the outlet. The tube is arranged horizontally and the effect of gravity is ignored. The tube inner wall and surface of the inserts are set as no slip surfaces.

$$C_p = (1870 + 3.692T)\mathrm{Jkg^{-1}K^{-1}} \tag{4}$$

$$\rho = (878.48 - 0.6525T)\mathrm{kgm^{-3}} \tag{5}$$

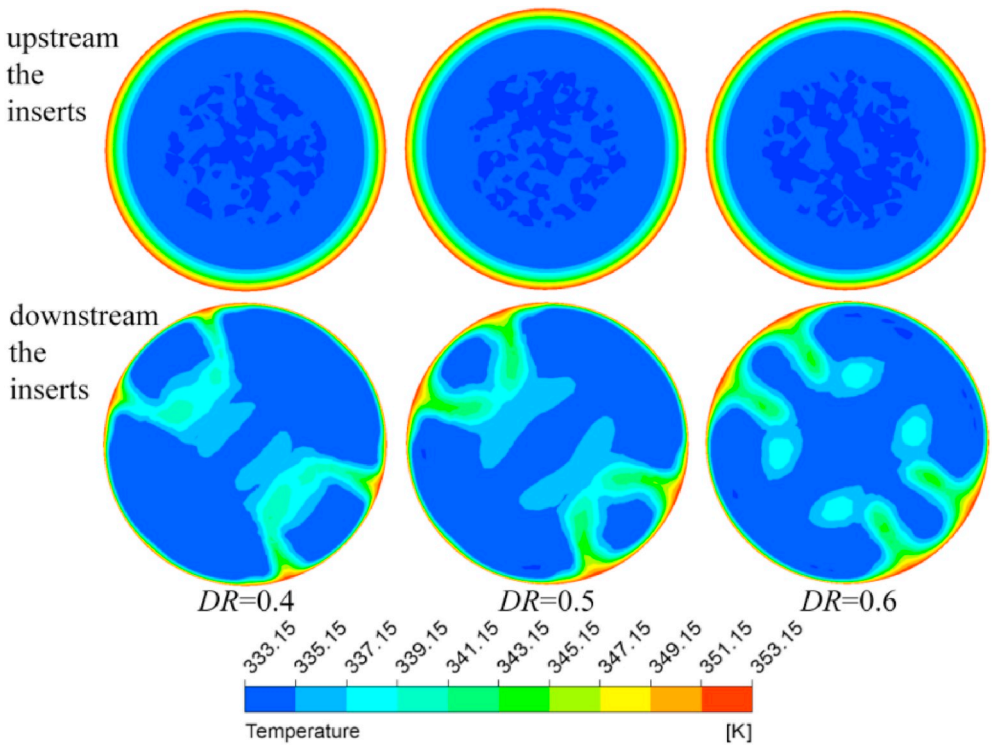

Fig. 4. Temperature contours of cross-sections before and after the inserts at $Re = 300$ and $N = 4$.

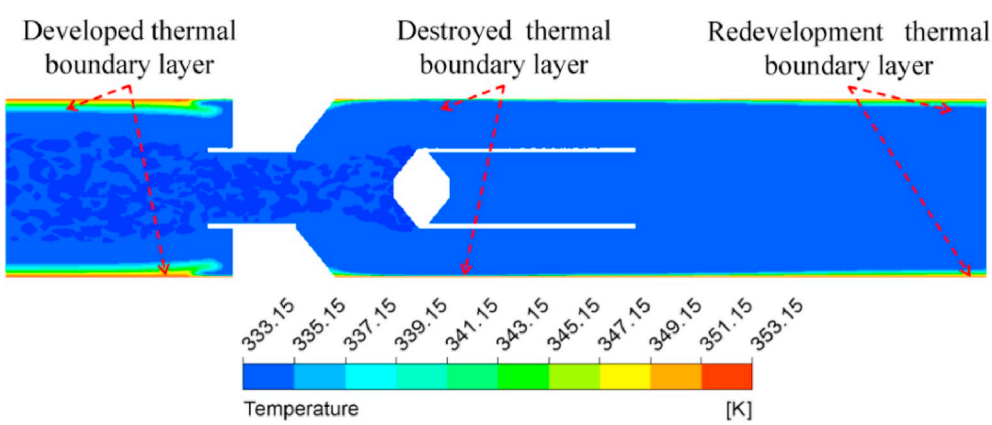

Fig. 5. Local temperature contour of axial section at $Re = 300$, $N = 4$ and $DR = 0.4$.

$$\mu/\rho = \exp\left(5.4628 - 5.9653 \times 10^{-2}T + 2.5938 \times 10^{-4}T^2 - 4.4743 \times 10^{-7}T^3\right) \times 10^{-6} \ \mathrm{m^2s^{-1}} \tag{6}$$

$$\lambda = \left(0.1326 - 7.42 \times 10^{-5}T\right) \ \mathrm{Wm^{-1}K^{-1}} \tag{7}$$

3.2. Computation parameters

In this study, the computation parameters, including Reynolds number (Re), average heat transfer coefficient (h), Nusselt number (Nu) and friction factor (f), are defined as Eqs. (8)–(11):

$$Re = \frac{\rho u D}{\mu} \tag{8}$$

$$h = \frac{q}{T_w - T_m} \tag{9}$$

$$Nu = \frac{hD}{\lambda} \tag{10}$$

$$f = \frac{\Delta P}{(L/D)\rho u^2/2} \tag{11}$$

where u is the mean velocity on the cross-sectional plane, T_w and T_m is the average temperature of the tube wall and the fluid, and ΔP is the pressure difference between the inlet and the outlet.

3.3. Grid system and independence study

The three-dimensional grid system was generated by commercial software Gambit 2.4.6. For the domain without inserts, hexahedral mesh with highly refined grid near the tube wall was applied, as the mesh of cross-section A-A shows in Fig. 3. For the domain with insert, unstructured cells were adopted. In addition, to accurately reveal the flow and heat transfer characteristics of the boundary layer, highly refined grid with prismatic cells was applied to the region near tube wall. In the region near the fluid exchanger inserts, local grid refinement is used. Hex core mesh was adopted in the core region to improve the simulation

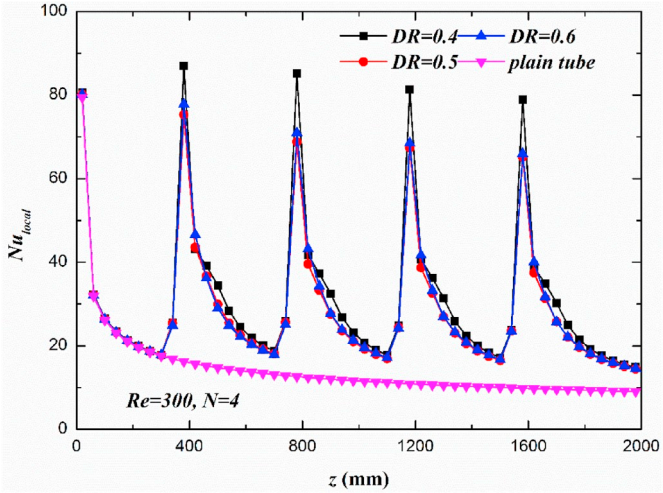

Fig. 6. Local Nusselt numbers along flow direction at $Re = 300$ and $N = 4$ for different diameter ratios and plain tube.

accuracy. Tetrahedrons and rectangular pyramids were applied for the transition from the prismatic cells to hex core meshes. As the mesh of cross-section B-B shows in Fig. 3.

In order to confirm mesh independence and to yield accurate computational results with the least number of elements, three mesh models (model-Imodel-II and model-III) for $DR = 0.5$, $N = 4$ at $Re = 300$, were used for discretizing the interior domain of tube fitted with fluid exchanger inserts. The values of Nu and f obtained from converged solution and errors of Nu and f between different mesh models were listed in Table 1. The result showed that obvious error existed between model-I and model-II, while deviations of Nu and f between model-II and model-III were considerably limited. Therefore, it was concluded that mesh model-II was the denser mesh for this simulation. After grid independence test, all computations are run with the mesh model-II.

3.4. Calculation method and validation

In this study, the commercial software ANSYS FLUENT 16.0 was used for CFD computations. Laminar model is adopted and the second-order upwind discretization scheme is applied in the present study. For coupling the velocity and pressure in the calculation, SIMPLE algorithm was employed. Moreover, the convergence criterion is set such that the residual of energy is less than 10^{-7} and the residuals of other parameters are less than 10^{-4}. It takes about 24 h for one case to reach the convergence criterion on a 12-intel-core computer with a RAM memory of 8 GB.

To validate the reliability of the numerical model, comparisons between calculation results and values predicted by correlations for Nu and f are conducted and listed in Table 2. Eq. (12) [16] is the Sieder-Tate correlation for Nu under laminar flow when considering the inlet effect, which is obtained through the induction of a large amount of experiment data by E.N. Sieder and G.E. Tate [36]. Eq. (13) is the correlation of theoretical values for fully developed tube flow. The results indicate that deviations of Nu between the numerical results and the values predicted by Eq. (12) are limited in −15.7%, which are within the prediction accuracy range of the correlation (±20%). Meanwhile, the calculation values of f of are 2.6–10.2% larger than the theoretical values. And this is reasonable that the flow resistance of tube flow with inlet effect is slightly higher than that of the fully developed tube flow. Therefore, the calculation model has reasonable reliability.

$$Nu = 1.86\left(\frac{Re_f \quad Pr_f}{L/D}\right)^{1/3}\left(\frac{\mu_f}{\mu_w}\right)^{0.14} \tag{12}$$

$$f = 64/Re \tag{13}$$

4. Results and discussion

4.1. Heat transfer

Fig. 4 displays the temperature contours on cross-sections 20 mm

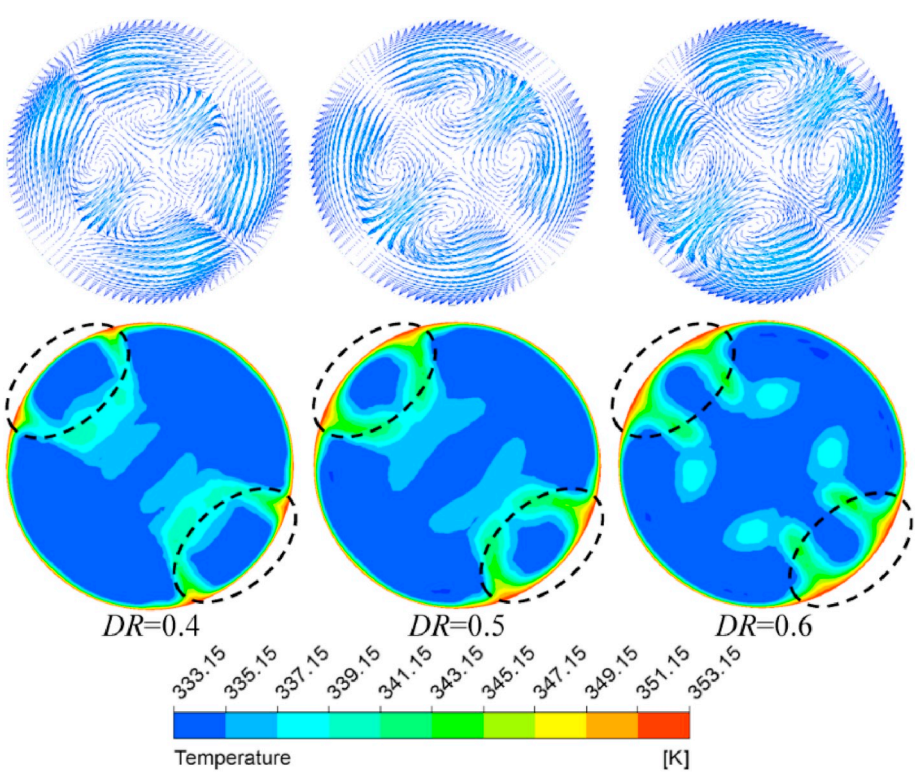

Fig. 7. Tangential vector and temperature contours for different *DRs*.

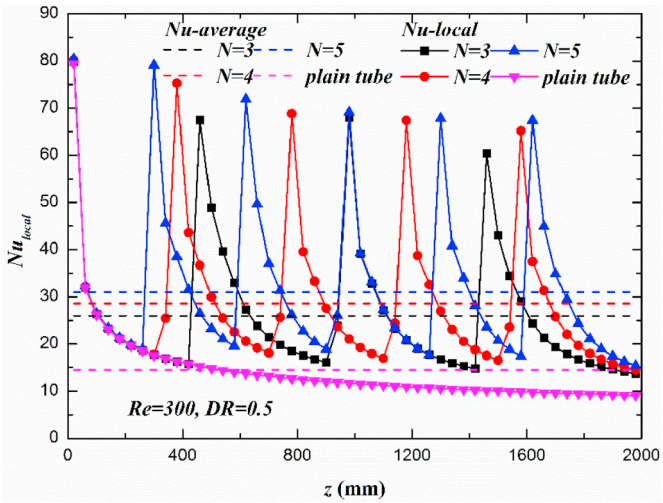

Fig. 8. Local Nusselt numbers along flow direction at $Re = 300$ for different number of inserts and plain tube.

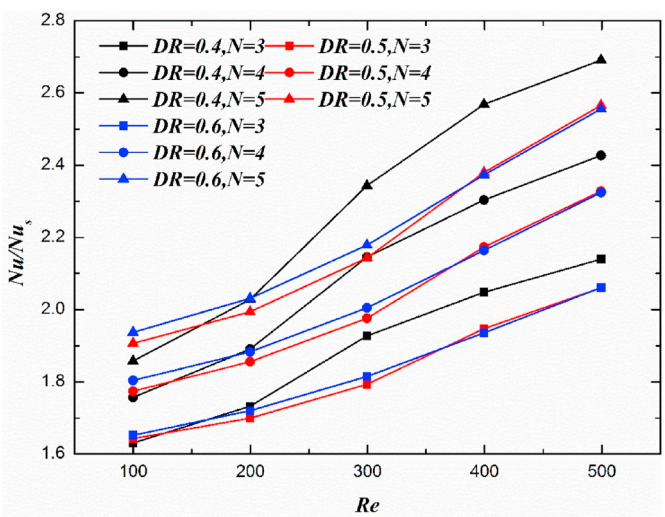

Fig. 9. Effects of parameters on the Nu/Nu_s ratio.

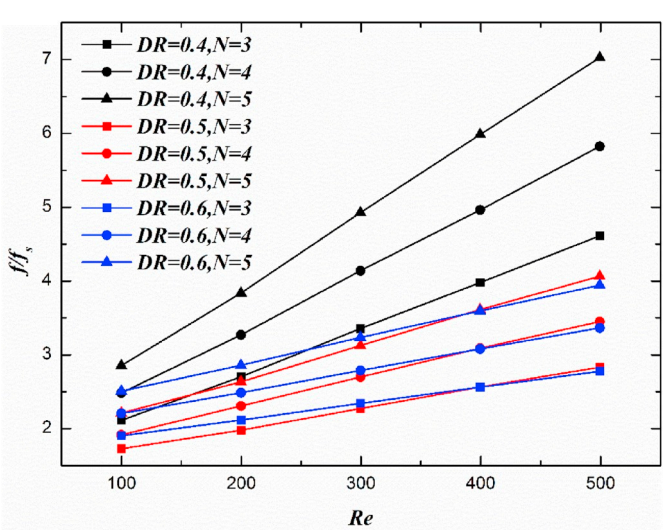

Fig. 10. Effects of parameters on the f/f_s ratio.

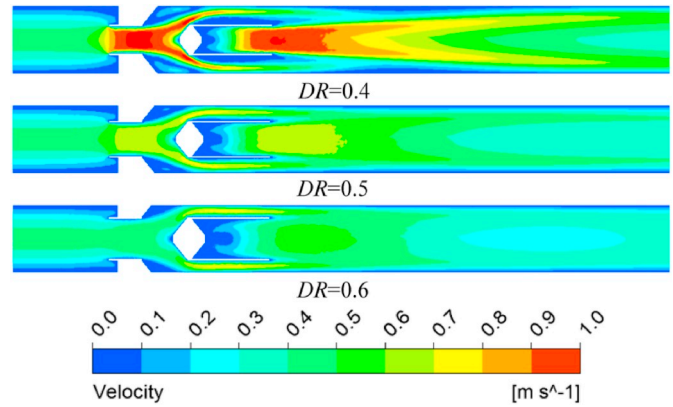

Fig. 11. Velocity contours on the axial section for different diameter ratios at $Re = 300$.

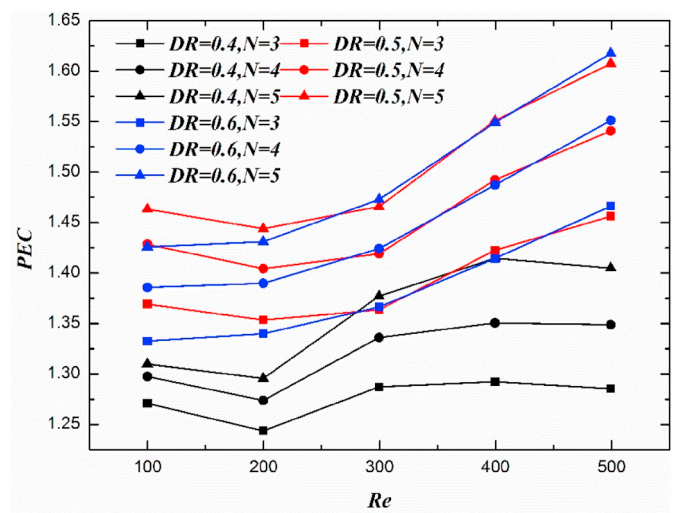

Fig. 12. Variation of *PEC* with *Re*.

upstream and downstream the inserts at $Re = 300$ and $N = 4$ for different *DR*. It is clearly seen that after the developed flow going through the fluid exchanger inserts, the cold fluid in the core region of the tube is exchanged to the boundary and the thermal boundary layer is completely destroyed. Therefore, the heat transfer in the tube downstream the fluid exchanger inserts will be dramatically enhanced. Local temperature contour of axial section at $Re = 300$, $N = 4$ and $DR = 0.4$ is presented in Fig. 5 to analyze the change of thermal boundary along the flow direction. From Fig. 5, we can see that the developed thermal boundary layer upstream the inserts is completely destroyed after the fluid passing the inserts and then the thermal boundary redevelops until it reaches to the next fluid exchanger inserts and destroyed again. As a result, the thermal boundary layer can be periodically destroyed and consequently the heat transfer can be effectively improved.

Fig. 6 shows the Local Nusselt numbers along flow direction at $Re = 300$ and $N = 4$ for different diameter ratios and plain tube. For the plain tube, as the thermal boundary layer develops, the local Nusselt number decreases rapidly near the tube inlet and then becomes more and more gradual along the flow direction. Moreover, it is concluded that the formation and development of thermal boundary layers will reduce heat transfer performance drastically, especially in the early stages of the formation of the thermal boundary layer. For the enhanced tubes fitted with fluid exchanger inserts, from the inlet to the first fluid exchanger inserts, the local Nusselt numbers perform the same trend as that of the plain tube. However, after the fluid passing through the first inserts, the

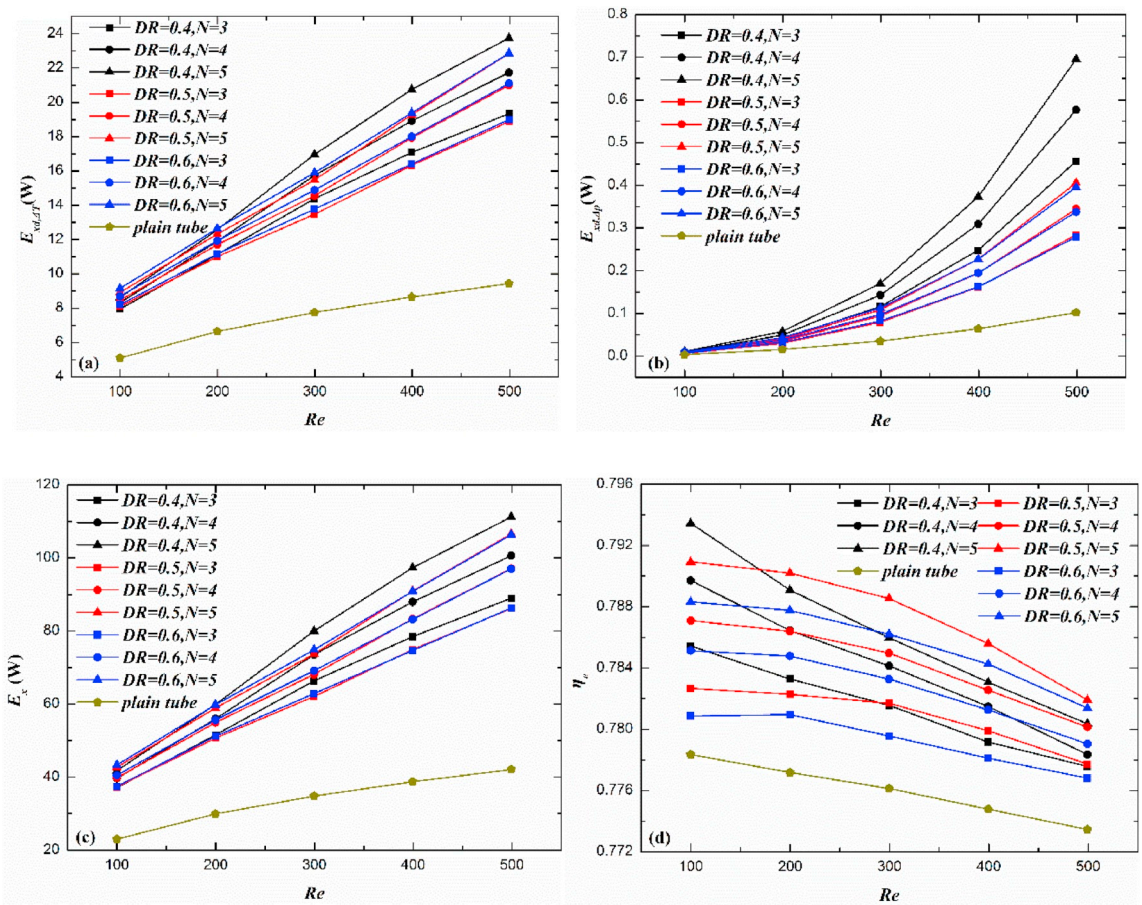

Fig. 13. Variations of thermal dissipation, power consumption, total exergy flux and exergy efficiency (η_e) with *Re*.

local Nusselt numbers are renewed to values close to that of the entrance, and then the local Nusselt numbers decrease rapidly again until the fluid passes through the next inserts. This indicates that when the fluid passes through the first inserts, the thermal boundary layer is completely destroyed and then re-generates and re-develops until destroyed by the next inserts. Thus, the local Nusselt numbers of tubes fitted with fluid exchanger inserts present periodic zigzag distribution along the flow direction. In addition, compared to the plain tube, the average Nusselt number is effectively enhanced. Moreover, we can observe that the local Nusselt numbers of the enhanced tube with $DR = 0.4$ is better than that of the enhanced tubes with $DR = 0.5$ and 0.6. Tangential vectors and temperature contours on the cross-section 20 mm downstream of the inserts are presented in Fig. 7, which helps to analyze the mechanism of this phenomenon. It is observed that two pairs of longitudinal vortexes are formed downstream of the inserts. These longitudinal vortexes bring the cold fluid in the area marked by black dotted circle, which has been exchanged to the region near the tube wall by the inserts, back to the core region of the tube and perform a negative effect on the heat transfer enhancement. In addition, as the *DR* decreases, the size of the vortex decreases. Thus, in the case of $DR = 0.4$, less cold fluid in the area marked by black dotted circle is carried away from the tube wall and the average Nusselt number is higher than that of the cases with $DR = 0.5$ and 0.6.

Fig. 8 presents the local Nusselt numbers at $Re = 300$ and $DR = 0.5$ for different numbers of inserts and plain tube. Similarly, it is clear that the local Nusselt numbers of the enhanced tubes perform periodic zigzag distributions, and the number of zigzags is the same as the number of fluid exchanger inserts. Furthermore, the average Nusselt number increases with the number of fluid exchanger inserts, as the dash lines show in Fig. 8. Fig. 9 illustrates the total Nusselt number ratios (Nu/Nu_s) between the enhanced tubes and plain tube along with *Re* number. The result indicates that the Nu/Nu_s ratio, which ranges from 1.63 to 2.69, increases with the number of inserts and *Re* number. The Nu/Nu_s ratio increases with the diameter ratio (*DR*) at lower *Re* number ($Re < 200$) but presents the opposite trend at higher *Re* number ($Re > 200$). In addition, when at high *Re* number ($Re \geq 300$), the differences of the Nu/Nu_s ratio between cases with $DR = 0.5$ and 0.6 are limited and their total Nu/Nu_s ratios are much lower than those of cases with $DR = 0.4$.

4.2. Flow resistance

Considering that the flow resistance is an important parameter of HTET, which is related to the operating pumping power cost, Fig. 10 displays the friction factor ratios (f/f_s) between the enhanced tubes and plain tube along with *Re* number. The result indicates that the f/f_s ratio ranges from 1.72 to 7.01 and increases with the number of fluid exchanger inserts and *Re* number. The friction factors of the cases with smaller diameter ratio (*DR*) increase faster with *Re* number than those of cases with larger diameter ratio (*DR*). Moreover, there is little difference of flow resistance between $DR = 0.5$ and 0.6, but the f/f_s ratios of cases with $DR = 0.4$ are much higher than those of cases with $DR = 0.5$ and 0.6. It is because when $DR = 0.4$, a high-speed flow area is formed in the central circular channel of the heat exchanger inserts due to the throttling effect, as shown in Fig. 11.

4.3. The overall thermo-hydraulic performance

In this study, the performance evaluation criterion (*PEC*), which reflects the enhancement of heat transfer performance under given pimping power [37], is employed to appraise the overall

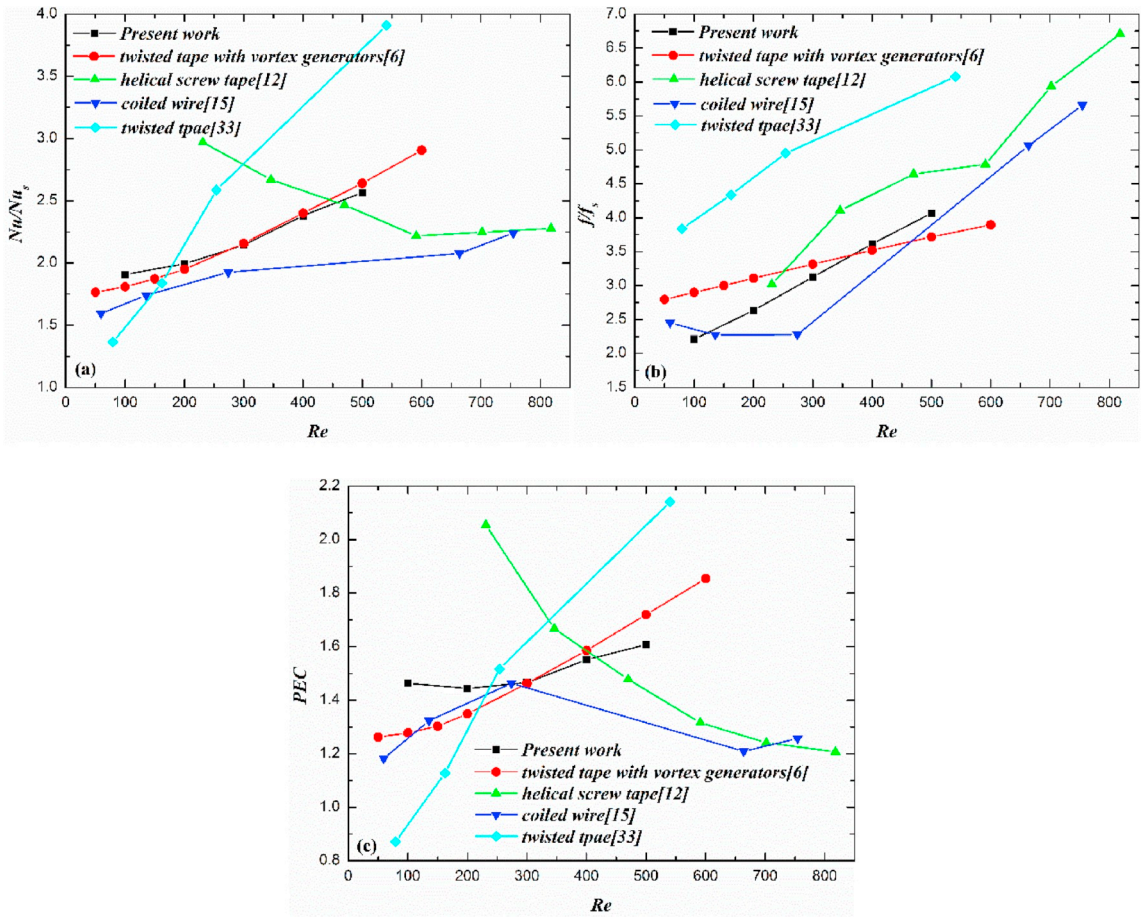

Fig. 14. Comparison with the previous published works: (a) Nu/Nu_s ratio; (b) f/f_s ratio; (c) *PEC*.

thermal-hydraulic performance of the tube with fluid exchanger inserts. The definition of *PEC* is written as follow:

$$PEC = \frac{Nu/Nu_s}{(f/f_s)^{1/3}} \tag{14}$$

where Nu_s and f_s represent the *Nu* and *f* of the plain tube under the same Reynolds number, respectively.

Fig. 12 illustrates the *PEC* value with *Re* number. From Fig. 12, it is observed that the *PEC* values of tube with fluid exchanger inserts range from 1.24 to l.62 and increase with the number of inserts. Moreover, the *PEC* values of cases with $DR = 0.4$ are much lower than those of cases with $DR = 0.5$ and 0.6 due to its large flow resistance mentioned above. When $Re < 300$, the cases with $DR = 0.5$ obtains the highest *PEC* value, while the difference of *PEC* value between cases with $DR = 0.5$ and 0.6 is limited when $Re \geq 300$.

4.4. Exergy analysis

Exergy analysis is conducted to appraise the thermodynamic performance of the tube with fluid exchanger inserts. According to Liu's research [38], thermal dissipation and power consumption, which are defined as Eqs. (15) and (16), are two sources of total exergy destruction. And the total exergy flux loaded on the boundary is expressed as Eq. (17), in which T_0 and T are the ambient temperature (293.15 K) and temperature of tube wall, respectively. The exergy efficiency of the convective heat transfer in the tube is written as Eq. (18) below.

$$E_{xd,\Delta T} = \iiint_{\Omega} T_0 \frac{\lambda(\nabla T)^2}{T^2} dV \tag{15}$$

$$E_{xd,\Delta p} = \iiint_{\Omega} \mathbf{U} \cdot \left(\rho \mathbf{U} \cdot \nabla \mathbf{U} - \mu \nabla^2 \mathbf{U}\right) dV \tag{16}$$

$$E_x = \iiint_{\Omega} -\nabla \cdot \left[\left(1 - \frac{T_0}{T}\right)\mathbf{q}\right] dV \tag{17}$$

$$\eta_e = 1 - \frac{E_{xd,\Delta T} + E_{xd,\Delta p}}{E_x} \tag{18}$$

Variations of thermal dissipation, power consumption, total exergy flux and exergy efficiency with *Re* number for enhanced tubes and plain tube are presented in Fig. 13. From Fig. 13 (a) and (c), thermal dissipation and total exergy flux perform the similar trend. Both of them increase with the number of inserts and *Re* number, and the values of cases with $DR = 0.4$ are larger than those of cases with $DR = 0.5$ and 0.6. In addition, both the thermal dissipation and total exergy flux of enhanced tube are larger than those of plain tube. Fig. 13 (b) indicates that the power consumptions of enhanced tubes are much larger than those of plain tube, and increase sharply with *Re* number. Furthermore, effects of parameters on the power consumption perform the same trend as the f/f_s ratio in Fig. 10. From Fig. 13 (d), it is found that exergy efficiencies of both the plain tube and the enhanced tube decrease with the increasing *Re* number, and compared to the plain tube, the exergy efficiency of the enhanced tube is improved by 0.3%–1.9%. Moreover, as the diameter ratio decreases, the exergy efficiency decreases faster with the increasing *Re* number. In addition, the exergy efficiency increases with the number of fluid exchanger inserts and the cases with moderate diameter ratio ($DR = 0.5$) obtain the highest exergy efficiency when $Re > 100$.

4.5. Comparison with previous works

The comparison with the previous published works, including twisted tape with vortex generators [6], helical screw tape [12], coiled wire [15] and twisted tape [33], are displayed in Fig. 14 (a)–(c). It is clear that both Nu/Nu_s ratio and f/f_s ratio of the present work are larger than that of coiled wire, and the present work obtains a higher overall thermal-hydraulic performance than coiled wire. Compared to other works, the present work obtains moderate heat transfer performance and low pressure drop, and consequently gains high *PEC* value, especially at low Reynolds number. Therefore, the proposed idea is suitable for applications with high viscosity fluid at low Re number. In this study, a 2 m long tube fitted with only 5 fluid exchanger inserts can obtain heat transfer performance equivalent to tube with a full-length twisted tape. Thus, compared with twisted tape, the fluid exchanger insert has advantages in saving materials.

5. Conclusions

A novel fluid exchanger inserts is proposed and numerically investigated for enhancing convective heat transfer of laminar oil flow in a circular tube. Effects of parameters (diameter ratio and number of inserts) on thermal-hydraulic performance are also investigated. Detailed description and analysis of heat transfer and pressure drop are carried out in this study. Moreover, exergy analysis is conducted to appraise the thermodynamic performance. According to numerical results, conclusions are drawn as follows:

(1) The fluid exchanger inserts can completely interchange the cold fluid in the center of the tube and the hot fluid in the boundary. Therefore, it can completely destroy the thermal boundary layer periodically and effectively enhance the heat transfer.
(2) The tube fitted with fluid exchanger inserts obtains a considerable augmentation in heat transfer. The *Nu* of the enhanced tube ranges from 16.58 to 46.16, which is 1.63–2.69 times that of the plain tube. The *f* of the enhanced tube is increased to 1.72–7.01 times that of the plain tube. Both the Nu/Nu_s ratio and f/f_s ratio increase with the number of inserts. The *Nu* and *f* of cases with $DR = 0.4$ are much higher than that of cases with $DR = 0.5$ and 0.6 but the differences of *Nu* and *f* between cases with $DR = 0.5$ and 0.6 are small. The thermal-hydraulic performance (*PEC* value) of tube with fluid exchanger inserts ranges from 1.24 to l.62 and increases with the number of inserts. The cases with $DR = 0.5$ and 0.6 have the similar PEC values which are much higher than that of cases $DR = 0.4$.
(3) Compared to the plain tube, the exergy efficiency of the enhanced tube is improved by 0.3%–1.9%. The exergy efficiency increases with the number of fluid exchanger inserts and decreases with *Re* number. Moreover, the cases with moderate diameter ratio ($DR = 0.5$) obtain the highest exergy efficiency when $Re > 100$.

Declaration of competing interest

To the best of our knowledge and belief, neither I nor any coauthors have any possible conflicts of interest.

Acknowledgment

The work was supported by the National Natural Science Foundation of China (Grant No. 51736004).

References

[1] R.L. Webb, N.-H. Kim, Principle of Enhanced Heat Transfer, Taylor Francis, New York, NY, USA, 1994.
[2] N. Zheng, F. Yan, K. Zhang, T. Zhou, Z. Sun, A review on single-phase convective heat transfer enhancement based on multi-longitudinal vortices in heat exchanger tubes, Appl. Therm. Eng. 164 (2020) 114475.
[3] R. Manglik, A. Bergles, Heat transfer and pressure drop correlations for twisted-tape inserts in isothermal tubes: part I–laminar flows, Trans. Am. Soc. Mech. Eng. J. Heat Trans. 115 (1993), 881-881.
[4] R.M. Manglik, A.E. Bergles, Heat transfer and pressure drop correlations for twisted-tape inserts in isothermal tubes: Part II—transition and turbulent flows, J. Heat Tran. 115 (4) (1993) 890–896.
[5] S.K. Saha, A. Dutta, S.K. Dhal, Friction and heat transfer characteristics of laminar swirl flow through a circular tube fitted with regularly spaced twisted-tape elements, Int. J. Heat Mass Tran. 44 (22) (2001) 4211–4223.
[6] J. Guo, A. Fan, X. Zhang, W. Liu, A numerical study on heat transfer and friction factor characteristics of laminar flow in a circular tube fitted with center-cleared twisted tape, Int. J. Therm. Sci. 50 (7) (2011) 1263–1270.
[7] Z.-M. Lin, L.-B. Wang, M. Lin, W. Dang, Y.-H. Zhang, Numerical study of the laminar flow and heat transfer characteristics in a tube inserting a twisted tape having parallelogram winglet vortex generators, Appl. Therm. Eng. 115 (2017) 644–658.
[8] Y. He, L. Liu, P. Li, L. Ma, Experimental study on heat transfer enhancement characteristics of tube with cross hollow twisted tape inserts, Appl. Therm. Eng. 131 (2018) 743–749.
[9] A. Saysroy, S. Eiamsa-ard, Periodically fully-developed heat and fluid flow behaviors in a turbulent tube flow with square-cut twisted tape inserts, Appl. Therm. Eng. 112 (2017) 895–910.
[10] P. Murugesan, K. Mayilsamy, S. Suresh, P. Srinivasan, Heat transfer and pressure drop characteristics in a circular tube fitted with and without V-cut twisted tape insert, Int. Commun. Heat Mass Tran. 38 (3) (2011) 329–334.
[11] S.W. Chang, T.L. Yang, J.S. Liou, Heat transfer and pressure drop in tube with broken twisted tape insert, Exp. Therm. Fluid Sci. 32 (2) (2007) 489–501.
[12] S.W. Chang, Y.J. Jan, J.S. Liou, Turbulent heat transfer and pressure drop in tube fitted with serrated twisted tape, Int. J. Therm. Sci. 46 (5) (2007) 506–518.
[13] P. Sivashanmugam, S. Suresh, Experimental studies on heat transfer and friction factor characteristics of laminar flow through a circular tube fitted with helical screw-tape inserts, Appl. Therm. Eng. 26 (16) (2006) 1990–1997.
[14] X. Zhang, Z. Liu, W. Liu, Numerical studies on heat transfer and friction factor characteristics of a tube fitted with helical screw-tape without core-rod inserts, Int. J. Heat Mass Tran. 60 (2013) 490–498.
[15] E.Z. Ibrahim, Augmentation of laminar flow and heat transfer in flat tubes by means of helical screw-tape inserts, Energy Convers. Manag. 52 (1) (2011) 250–257.
[16] M.A. Akhavan-Behabadi, R. Kumar, M.R. Salimpour, R. Azimi, Pressure drop and heat transfer augmentation due to coiled wire inserts during laminar flow of oil inside a horizontal tube, Int. J. Therm. Sci. 49 (2) (2010) 373–379.
[17] Y. Hong, J. Du, S. Wang, S.-M. Huang, W.-B. Ye, Heat transfer and fluid flow behaviors in a tube with modified wire coils, Int. J. Heat Mass Tran. 124 (2018) 1347–1360.
[18] O. Keklikcioglu, V. Ozceyhan, Experimental investigation on heat transfer enhancement in a circular tube with equilateral triangle cross sectioned coiled-wire inserts, Appl. Therm. Eng. 131 (2018) 686–695.
[19] Z. Sun, K. Zhang, W. Li, Q. Chen, N. Zheng, Investigations of the turbulent thermal-hydraulic performance in circular heat exchanger tubes with multiple rectangular winglet vortex generators, Appl. Therm. Eng. 168 (2020) 114838.
[20] Y. Lei, F. Zheng, C. Song, Y. Lyu, Improving the thermal hydraulic performance of a circular tube by using punched delta-winglet vortex generators, Int. J. Heat Mass Tran. 111 (2017) 299–311.
[21] A.T. Wijayanta, I. Yaningsih, M. Aziz, T. Miyazaki, S. Koyama, Double-sided delta-wing tape inserts to enhance convective heat transfer and fluid flow characteristics of a double-pipe heat exchanger, Appl. Therm. Eng. 145 (2018) 27–37.
[22] S. Skullong, P. Promvonge, C. Thianpong, N. Jayranaiwachira, M. Pimsarn, Thermal performance of heat exchanger tube inserted with curved-winglet tapes, Appl. Therm. Eng. 129 (2018) 1197–1211.
[23] X.W. Zhu, Y.H. Fu, J.Q. Zhao, A novel wavy-tape insert configuration for pipe heat transfer augmentation, Energy Convers. Manag. 127 (2016) 140–148.
[24] P. Liu, N. Zheng, F. Shan, Z. Liu, W. Liu, An experimental and numerical study on the laminar heat transfer and flow characteristics of a circular tube fitted with multiple conical strips inserts, Int. J. Heat Mass Tran. 117 (Supplement C) (2018) 691–709.
[25] M. Pourramezan, H. Ajam, Modeling for thermal augmentation of turbulent flow in a circular tube fitted with twisted conical strip inserts, Appl. Therm. Eng. 105 (2016) 509–518.
[26] A. Fan, J. Deng, A. Nakayama, W. Liu, Parametric study on turbulent heat transfer and flow characteristics in a circular tube fitted with louvered strip inserts, Int. J. Heat Mass Tran. 55 (19) (2012) 5205–5213.
[27] S. Eiamsa-ard, S. Pethkool, C. Thianpong, P. Promvonge, Turbulent flow heat transfer and pressure loss in a double pipe heat exchanger with louvered strip inserts, Int. Commun. Heat Mass Tran. 35 (2) (2008) 120–129.
[28] P.W. Deshmukh, S.V. Prabhu, R.P. Vedula, Heat transfer enhancement for laminar flow in tubes using curved delta wing vortex generator inserts, Appl. Therm. Eng. 106 (2016) 1415–1426.
[29] H.-l. Liu, H. Li, Y.-l. He, Z.-t. Chen, Heat transfer and flow characteristics in a circular tube fitted with rectangular winglet vortex generators, Int. J. Heat Mass Tran. 126 (2018) 989–1006.
[30] P. Li, P. Liu, Z. Liu, W. Liu, Experimental and numerical study on the heat transfer and flow performance for the circular tube fitted with drainage inserts, Int. J. Heat Mass Tran. 107 (2017) 686–696.

[31] S. Chamoli, R. Lu, J. Xie, P. Yu, Numerical study on flow structure and heat transfer in a circular tube integrated with novel anchor shaped inserts, Appl. Therm. Eng. 135 (2018) 304–324.
[32] K. Nanan, C. Thianpong, M. Pimsarn, V. Chuwattanakul, S. Eiamsa-ard, Flow and thermal mechanisms in a heat exchanger tube inserted with twisted cross-baffle turbulators, Appl. Therm. Eng. 114 (2017) 130–147.
[33] W. Liu, P. Liu, Z.M. Dong, K. Yang, Z.C. Liu, A study on the multi-field synergy principle of convective heat and mass transfer enhancement, Int. J. Heat Mass Tran. 134 (2019) 722–734.
[34] W. Tu, Y. Tang, J. Hu, Q. Wang, L. Lu, Heat transfer and friction characteristics of laminar flow through a circular tube with small pipe inserts, Int. J. Therm. Sci. 96 (2015) 94–101.
[35] S.K. Agarwal, M. Raja Rao, Heat transfer augmentation for the flow of a viscous liquid in circular tubes using twisted tape inserts, Int. J. Heat Mass Tran. 39 (17) (1996) 3547–3557.
[36] G.E.T.E.N. Seider, Heat transfer and pressure drop of liquid in tubes, Ind. Eng. Chem. 28 (12) (1936) 1429–1435.
[37] R. Webb, Performance evaluation criteria for use of enhanced heat transfer surfaces in heat exchanger design, Int. J. Heat Mass Tran. 24 (4) (1981) 715–726.
[38] W. Liu, P. Liu, J.B. Wang, N.B. Zheng, Z.C. Liu, Exergy destruction minimization: a principle to convective heat transfer enhancement, Int. J. Heat Mass Tran. 122 (2018) 11–21.